High-Efficiency and Radiated EMI Reduction Technology for WPT Systems Using Soft-switching Active Bridge Converter

Ryohei Okada[1)*], **Ryosuke Ota**[2)], **Nobukazu Hoshi**[1)]

1)*Tokyo University of Science, Faculty of Science and Technology, Chiba, Japan*
2)*Tokyo Metropolitan University, Faculty of System Design, Tokyo, Japan*
[*]*E-mail: r_okada@alumni.tus.ac.jp*

ABSTRACT: In wireless power transfer systems, applying a soft-switching technology increases power losses from reactive currents circulating in the circuit, reducing overall efficiency. To address this problem, the authors have proposed a soft-switching active bridge converter. The proposed converter utilizes the reactive current generated in an auxiliary circuit (LC circuit) for soft switching instead of a resonant network. This approach significantly reduces the reactive current flowing through the resonant network and power devices. This paper summarizes the authors' previous findings on the proposed converter and presents the efficiency improvement method. Experimental results have shown that the proposed system achieves higher efficiency than the conventional system with soft switching while reducing radiated EMI compared to the conventional system with hard switching.

KEY WORDS: Wireless power transfer, soft switching, high efficiency, electromagnetic noise, active bridge converter.

I. Introduction

Wireless power transfer (WPT) technology is expected to be a means to extend the driving range of electric vehicles [1]–[4]. Currently, there is a growing demand for increased power output in WPT systems to facilitate dynamic charging and rapid charging. However, the increase in system capacity brings challenges, including power conversion losses and radiated electromagnetic noise (EMI) caused by the switching of semiconductor power devices.

Soft-switching technology is a method to reduce the switching losses and radiated EMI of power devices. In traditional WPT systems, soft switching is achieved using reactive current generated by a resonant network [5]–[8]. However, the reactive current circulates throughout the system, leading to significant efficiency drops due to conduction losses [9]–[12]. To address this issue, the authors have proposed a soft-switching active bridge converter, as shown in Fig. 1 [13]–[15]. The proposed converter generates the necessary reactive current for soft switching in an LC circuit connected to one leg of the converter, instead of in the resonant network. This reactive current flows only through one leg and the LC circuit, significantly reducing conduction losses.

This paper summarizes some of the authors' previous findings [14], [15] on the proposed converter and presents the efficient soft-switching technology.

II. Overview of Proposed System

A. Power Transmission with Proposed Converter

Fig. 1 shows the proposed WPT system with a double-sided LCC resonant network using the proposed converters. The LC circuits include inductors L_{LCp} and L_{LCs} [H], which generate reactive current and capacitors C_{LCp}, C_{LCs} [F], which block DC current.

In the proposed converters, the frequency and duty cycle of the switching are fixed at 85 kHz and 0.5, respectively. The primary- and secondary-side voltages v_{p} and v_{s} [V] in the resonant network are controlled by the phase-shift angles α_{p} and α_{s} [rad] between the legs. Furthermore, the transmission power P_{tr} [W] and reactive current are controlled by the phase-shift angle δ [rad] between v_{p} and v_{s}. These operations are the same as those in the conventional converters [5], [9].

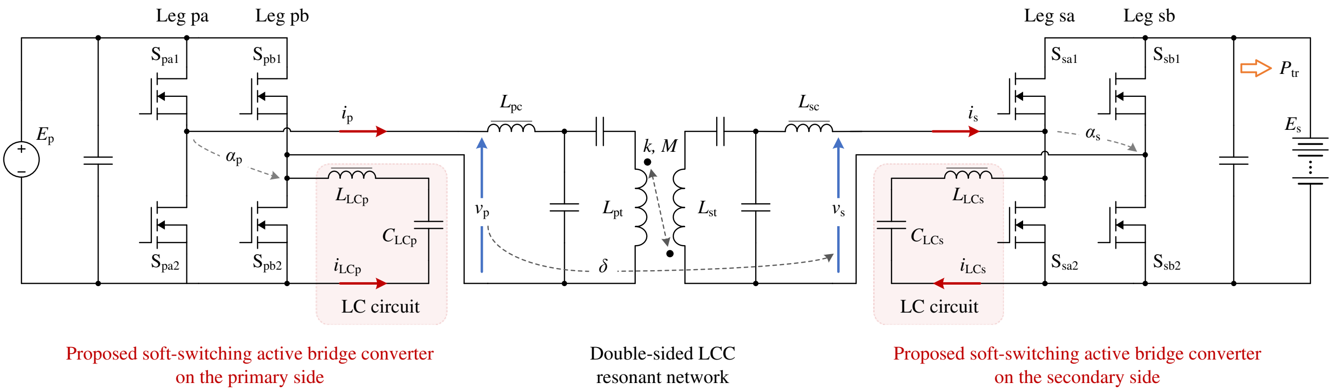

Fig. 1. Proposed WPT system with the soft-switching active bridge converters.

The transmission power P_{tr} can be expressed as

$$P_{\mathrm{tr}} = \frac{M|\boldsymbol{V}_{\mathrm{p}}||\boldsymbol{V}_{\mathrm{s}}|}{\omega L_{\mathrm{pc}} L_{\mathrm{sc}}} \cos\left(\frac{\pi}{2} - \delta\right), \tag{1}$$

where $\boldsymbol{V}_{\mathrm{p}}$ and $\boldsymbol{V}_{\mathrm{s}}$ [V] represent the phasor notations of the fundamental components of v_{p} and v_{s}, respectively. L_{pc}, L_{sc} and M [H] represent the compensation inductors and the mutual inductance between the transmission coils L_{pt} and L_{st} [H]. ω [rad/s] is the resonant angular frequency of the resonant network.

In addition, the maximum efficiency condition of the resonant network can be approximated by [14]

$$\begin{cases} \dfrac{|\boldsymbol{V}_{\mathrm{s}}|^2}{|\boldsymbol{V}_{\mathrm{p}}|^2} = \dfrac{r_{\mathrm{Lpt}} L_{\mathrm{sc}}^2 + r_{\mathrm{Lsc}} M^2}{r_{\mathrm{Lst}} L_{\mathrm{pc}}^2 + r_{\mathrm{Lpc}} M^2}, & (2) \\[2ex] \cos\left(\dfrac{\pi}{2} - \delta\right) = 1 \;\Leftrightarrow\; \delta = \dfrac{\pi}{2}, & (3) \end{cases}$$

where r_x [Ω] represents the equivalent series resistance (ESR) in each coil x. For simplicity, the ESRs in the compensation capacitors are not considered. Equation (2) represents the condition where the power losses due to $\boldsymbol{V}_{\mathrm{p}}$ and $\boldsymbol{V}_{\mathrm{s}}$ are balanced. In addition, (3) represents the condition where the fundamental power factor of the resonant network is unity, with minimized reactive current.

B. Soft-switching with Proposed Converter

Fig. 2 shows the typical operating waveforms of the primary-side proposed converter. E_{p} [V] represents the primary-side DC voltage, and i_{p} [A] is the primary-side current of the resonant network. $v_{\mathrm{L\_LCp}}$ [V] and i_{LCp} [A] denote the voltage and current of L_{LCp}, respectively. The operating waveforms on the secondary side are omitted, as they can be analyzed in the same way.

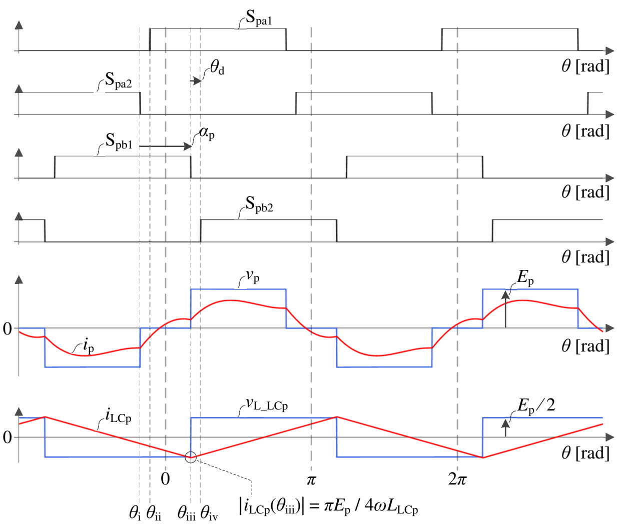

Fig. 2. Typical operating waveforms of the primary-side proposed converter.

Soft switching is achieved by turning on the power devices when the drain-source voltage is zero. For this, reverse current must flow through the power devices during the dead time period θ_{d} [rad] to discharge the charge of the output capacitance. This soft-switching condition can be expressed as

$$\begin{cases} i_{\mathrm{p}}\left(\theta_{\mathrm{i}}\right) \le 0 \\ i_{\mathrm{p}}\left(\theta_{\mathrm{ii}}\right) \le 0 \end{cases} \quad \text{for Leg pa,} \tag{4}$$

$$\begin{cases} i_{\mathrm{p}}\left(\theta_{\mathrm{iii}}\right) + i_{\mathrm{LCp}}\left(\theta_{\mathrm{iii}}\right) \le 0 \\ i_{\mathrm{p}}\left(\theta_{\mathrm{iv}}\right) + i_{\mathrm{LCp}}\left(\theta_{\mathrm{iv}}\right) \le 0 \end{cases} \quad \text{for Leg pb.} \tag{5}$$

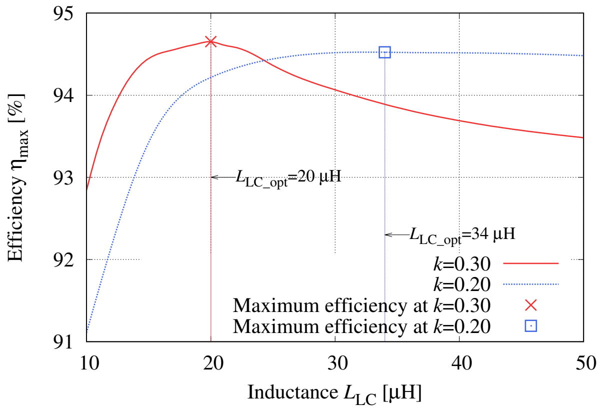

Fig. 3. Theoretical maximum-efficiency characteristics of the whole system at $P_{tr} = 2.5$ kW based on the analysis [14].

For the conventional converter to achieve soft switching, it must satisfy (5) with $i_{LCp} = 0$. In this case, δ must be controlled to meet (5), resulting in a low fundamental power factor in the resonant network and operation far from the efficiency-maximizing condition in (3). In contrast, the proposed converter can satisfy (5) while maintaining a high fundamental power factor by utilizing i_{LCp}.

C. Design Guideline for LC Circuits

Reducing L_{LCp} to increase $i_{LCp}(\theta)$ expands the soft-switching operation range that satisfies (3). However, since both the leg loss caused by i_{LCp} and the conduction loss in the LC circuit increase accordingly, the LC circuit must be designed considering these effects. Fig. 3 shows the maximum efficiency characteristics of the proposed system under soft-switching operating conditions. The efficiency $\eta_{max}(L_{LC})$ [%] in Fig. 3 represents the maximum efficiency point that satisfies (4) and (5). For simplicity, the analysis assumes $L_{LCp} = L_{LCs} = L_{LC}$. The optimal inductance value L_{LC_opt} in Fig. 3 corresponds to the point where $\eta_{max}(L_{LC})$ reaches its peak, satisfying the equality conditions of (3), (4), and (5). In other words, the proposed system achieves maximum efficiency when the reactive current in both the resonant and LC circuits is minimized.

However, as shown in Fig. 3, L_{LC_opt} is not constant; instead, it decreases as k increases. According to (1), a larger k results in greater transmission power P_{tr}. To maintain P_{tr} at a constant value, the phase shift angles between the legs, α_p and α_s, must be increased, while the applied voltages $|\boldsymbol{V}_p|$ and $|\boldsymbol{V}_s|$ must be reduced. In this case, the instantaneous current $i_p(\theta_{iii})$ increases. Consequently, achieving soft-switching operation requires reducing L_{LC} and increasing $i_{LCp}(\theta_{iii})$.

However, this paper reports the results obtained when the system was designed with $L_{LC} = 34.0$ µH as a design guideline to minimize the losses caused by i_{LCp} and i_{LCs} [A]. In practical systems, the efficiency improvement can be enhanced by optimizing L_{LC} according to the operating range with the highest losses. However, the detailed design methodology for this optimization will be reported in the future.

III. Comparison between Proposed and Conventional Systems

This section demonstrates the effectiveness of the proposed system based on comparative results with the conventional system [14], [15].

Fig. 4 shows the whole-system efficiency characteristics of the proposed and conventional systems operating with soft switching, as derived from theoretical analysis [14]. The dotted lines represent points of maximum efficiency for each power level. As shown in Fig. 4, the proposed system expands the soft-switching operating range compared to the conventional system. This expansion increases the degree of freedom for δ, allowing it to be set closer to $\pi/2$ [rad] and resulting in a higher fundamental power factor of the resonant network. Consequently, the whole-system efficiency is improved significantly.

Fig. 5 shows the theoretical power-loss breakdowns of the proposed/conventional systems at $k = 0.2$. Fig. 5 presents a detailed loss analysis for each leg, based on the analytical parameters from [14]. In Fig. 5, P_{res} and P_{LC} [W] represent the conduction losses in the resonant network and the LC circuit, respectively. P_{x_con}, $P_{x\_sw(off)}$ [W], where x = pa, pb, sa, or sb, represent the conduction and turn-off losses in the legs pa, pb, sa, and sb, respectively. As shown in Fig. 5, the proposed system significantly reduces each loss compared to the conventional system. This improvement is attributed to the reduced reactive current in the resonant network. In addition, in the proposed converter, the currents i_{LCp} and i_{LCs} flow in the opposite direction to i_{p} and i_{s} [A] in legs pb and sa. As a result, the conduction losses in legs pb and sa, $P_{\mathrm{pb\_con}} + P_{\mathrm{sa\_con}}$, are significantly reduced. Furthermore, P_{LC} in the proposed system is extremely small compared to the total losses. Consequently, the proposed system achieves a significant reduction in total losses compared to the conventional system.

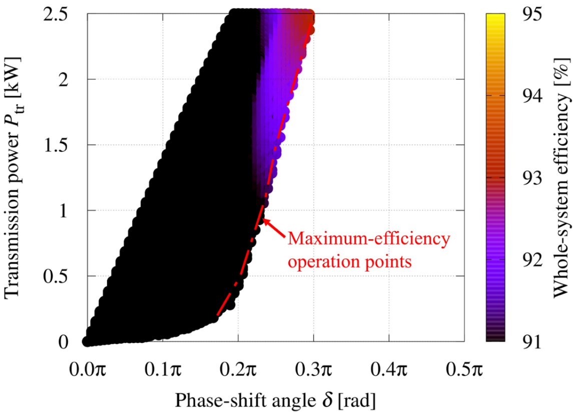

(a) Conventional system.

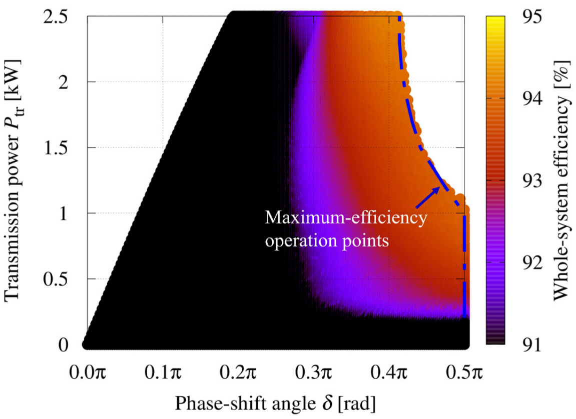

(b) Proposed system.

Fig. 4. Whole-system efficiency characteristics of the proposed system ($L_{\mathrm{LCp}} = L_{\mathrm{LCs}} = 34.0$ μH) and the conventional system, both controlled at $P_{\mathrm{tr}} = 2.5$ kW and operating with soft switching, based on theoretical analysis [14].

Fig. 6 illustrates the whole-system efficiency of the proposed and conventional systems in the experiments [14]. Each system operates at its maximum efficiency point, as shown in Fig. 4. As illustrated in Fig. 6, the proposed system achieves higher efficiency across a broader operating range

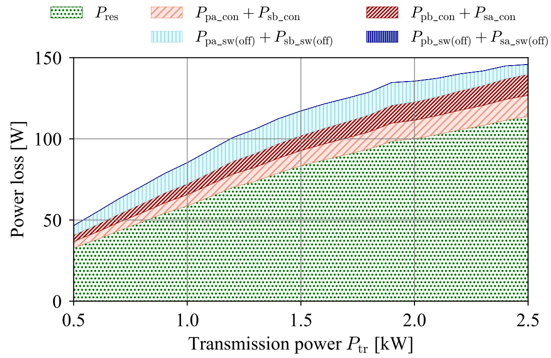

(a) Conventional system

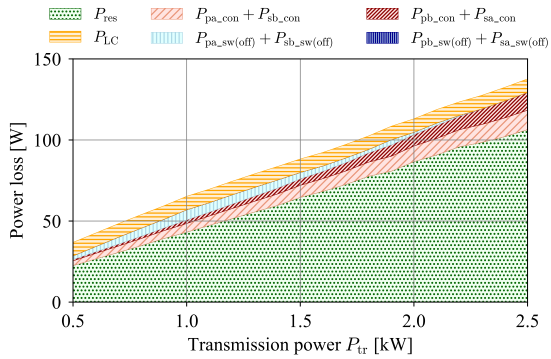

(b) Proposed system ($L_{\mathrm{LC}} = 34.0\ \mu$H)

Fig. 5. Theoretical power-loss breakdowns of the proposed/conventional systems at $k = 0.2$.

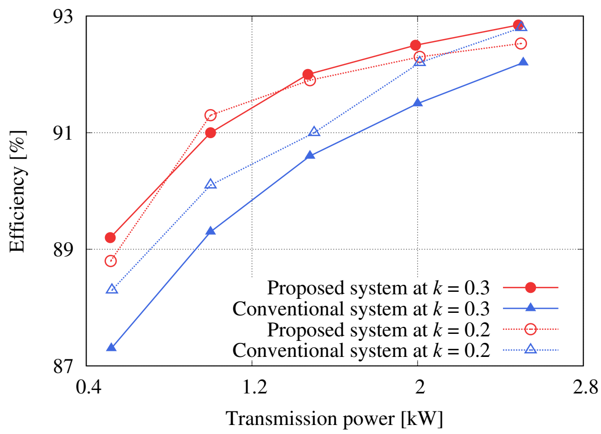

Fig. 6. Whole-system efficiency of the proposed system ($L_{\mathrm{LCp}} = L_{\mathrm{LCs}} = 34.0$ μH) and the conventional system in the experiments [14].

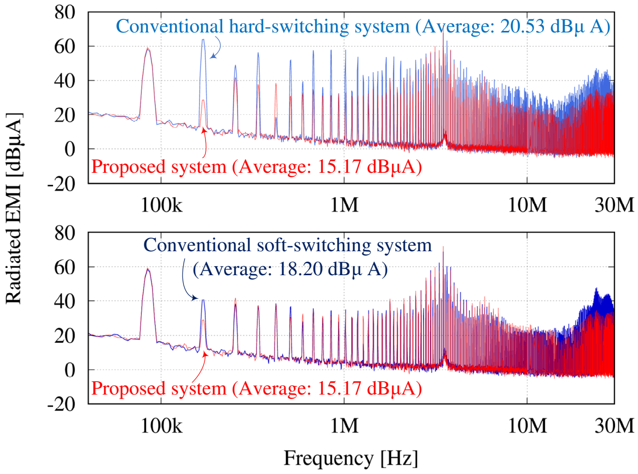

Fig. 7. Radiated EMI of the proposed system (L_{LCp}, L_{LCs} = 18.5, 30.2 μH) and the conventional systems, all controlled at $P_{\mathrm{tr}} = 2.5$ kW, in the experiments [15].

than the conventional system. Notably, when the coupling coefficient k between the transmission coils is high, the efficiency improvement becomes more pronounced. For example, with $k = 0.3$ and $P_{\mathrm{tr}} = 2.5$ kW, efficiency improved by 0.69 percentage points. According to (1), as k increases, it is necessary to increase α_{p} and α_{s} while decreasing $\boldsymbol{V}_{\mathrm{p}}$ and $\boldsymbol{V}_{\mathrm{s}}$ to maintain constant P_{tr}. In this situation, the conventional system requires decreasing δ from $\pi/2$ [rad] to satisfy (5), resulting in reduced efficiency. Therefore, the proposed system's advantages become more significant as k increases.

Fig. 7 shows the radiated EMI of the proposed and conventional systems controlled at $P_{\mathrm{tr}} = 2.5$ kW in the experiments [15]. "Conventional soft-switching system" is a system where the soft switching is applied to the conventional converter, while "Conventional hard-switching system" meets maximum efficiency conditions (2) and (3) but operates with hard switching. In Fig. 7, the proposed system achieves significant reduction in radiated EMI compared to the conventional hard-switching system, with an average reduction of 5.36 dBμA. This reduction is attributed to the reduction in radiated EMI originating from hard-switching operation. Additionally, the proposed system also reduces radiated EMI compared to the conventional soft-switching system, with an average reduction of 3.03 dBμA due to its ability to operate with a low current.

IV. Conclusion

This paper has presented an efficiency improvement method for WPT systems through a soft-switching active bridge converter. Experimental results have shown that the proposed system achieves higher efficiency than the conventional system with soft switching while reducing radiated EMI compared to the conventional system with hard switching. The proposed converter is particularly effective in systems requiring substantial reactive current for soft switching, such as those with large variations in coupling coefficient.

References

[1] K. Kusaka, K. Yamagata, J. Katsuya, and T. Sato, "Reduction in leakage magnetic flux of wireless power transfer systems with halbach coils," *IEEJ Journal of Industry Applications*, vol. 12, no. 6, pp. 1104–1105, 2023.

[2] E. Sato and K. Kondo, "Feasible power control method with a low sampling frequency for bidirectional wireless power transfer in battery-powered railway vehicle systems," *IEEJ Journal of Industry Applications*, vol. 12, no. 6, pp. 1078–1087, 2023.

[3] H. Ishida, T. Kyoden, and H. Furukawa, "Application of parity-time symmetry to low-frequency wireless power transfer system," *IEEJ Journal of Industry Applications*, vol. 11, no. 1, pp. 59–68, 2022.

[4] T. Fujita, Y. Deguchi, and H. Fujimoto, "Impedance analysis of parity-time wireless power transfer system using digital separate-oscillation," *IEEJ Journal of Industry Applications*, vol. 13, no. 6, pp. 703–710, 2024.

[5] X. Zhang, T. Cai, S. Duan, H. Feng, H. Hu, J. Niu, and C. Chen, "A control strategy for efficiency optimization and wide zvs operation range in bidirectional inductive power transfer system," *IEEE Transactions on Industrial Electronics*, vol. 66, no. 8, pp. 5958–5969, 2019.

[6] Y. Jiang, L. Wang, Y. Wang, J. Liu, X. Li, and G. Ning, "Analysis, design, and implementation of accurate zvs angle control for ev battery charging in wireless high-power transfer," *IEEE Transactions on Industrial Electronics*, vol. 66, no. 5, pp. 4075–4085, 2019.

[7] A. Namadmalan, "Self-oscillating pulsewidth modulation for inductive power transfer systems," *IEEE Journal of Emerging and Selected Topics in Power Electronics*, vol. 8, no. 2, pp. 1813–1820, 2020.

[8] H. Hu, T. Cai, S. Duan, X. Zhang, J. Niu, and H. Feng, "An optimal variable frequency phase shift control strategy for zvs operation within wide power range in ipt systems," *IEEE Transactions on Power Electronics*, vol. 35, no. 5, pp. 5517–5530, 2020.

[9] R. Ota, D. S. Nugroho, and N. Hoshi, “A consideration on maximum efficiency of resonant circuit of inductive power transfer system with soft-switching operation,” *World Electr. Veh. J.*, vol. 10, no. 3, 2019.

[10] N. Fu, J. Deng, Z. Wang, W. Wang, and S. Wang, “A hybrid mode control strategy for lcc–lcc- compensated wpt system with wide zvs operation,” *IEEE Transactions on Power Electronics*, vol. 37, no. 2, pp. 2449–2460, 2022.

[11] G. R. Kalra, B. S. Riar, and D. J. Thrimawithana, “An integrated boost active bridge based secondary inductive power transfer converter,” *IEEE Transactions on Power Electronics*, vol. 35, no. 12, pp. 12 716–12 727, 2020.

[12] G. Zhu, J. Dong, G. Yu, W. Shi, C. Riekerk, and P. Bauer, “Optimal multivariable control for wide output regulation and full-range efficiency optimization in lcc–lcc compensated wireless power transfer systems,” *IEEE Transactions on Power Electronics*, vol. 39, no. 9, pp. 11 834–11 848, 2024.

[13] R. Okada, R. Ota, and N. Hoshi, “Novel soft-switching active-bridge converter for bi-directional inductive power transfer system,” *IEEJ Journal of Industry Applications*, vol. 11, no. 1, pp. 97–107, 2022.

[14] R. Okada, R. Ota, and N. Hoshi, “Soft-switching converter for inductive power transfer system with double-sided lcc resonant network,” in *2022 24th European Conference on Power Electronics and Applications (EPE’22 ECCE Europe)*, 2022, pp. 1–11.

[15] R. Okada, R. Ota, and N. Hoshi, “Radiated emi reduction and efficiency improvement in wpt systems with passive auxiliary circuits for soft-switching,” in *2023 IEEE Transportation Electrification Conference and Expo, Asia-Pacific (ITEC Asia-Pacific)*, 2023, pp. 1–3.